Geophysical Research Letters
December 2008 ; Volume 35 (23) : Pages 1-5
http://dx.doi.org/10.1029/2008GL035635

An edited version of this paper was published by AGU.

Low-frequency variations of the large-scale ocean circulation and heat transport in the North Atlantic from 1955–1998 in situ temperature and salinity data

T. Huck[1, *], A. Colin de Verdière[1], P. Estrade[1] and R. Schopp[1]

[1] Laboratoire de Physique des Océans, UMR 6523 CNRS/IFREMER/IRD/UBO, Brest, France

*: Corresponding author : Huck T., email address : thierry.huck@univ-brest.fr

---

Abstract:

Low-frequency variations of the large-scale ocean circulation in the Atlantic are reconstructed from NODC pentadal anomalies of temperature and salinity from 1955 to 1998 based on hydrographic data, in addition to atmospheric reanalysis surface forcing. Diagnostic ocean circulations are estimated from simple methods using dynamical model integrations: namely diagnostic, robust diagnostic, and short prognostic. Mean transports of heat and mass are sensitive to the method and model configuration, but their decadal variability is much more coherent and does not depend explicitly on the variations of the surface forcing, its influence being imprinted in the thermohaline structure. Multidecadal variations are of the order of 20%, with large transports in the subpolar gyre in the early 1960's and mid 1990's, and low values in the mid 1970's. By reducing the influence of subgrid-scale parameterizations and surface forcings, these methods offer alternatives to exhaustive GCM simulations.

1. Introduction

Variations in the oceanic thermohaline structure have been documented over the last decades: surface intensified warming and changes in salinity, as well as deep water properties and formation rates [*Dickson et al.*, 1996, 2002]. However the associated changes in the large-scale ocean circulation are poorly known, and deserve much interest in the context of the ongoing global warming and possible decay of the thermohaline circulation [*Bryden et al.*, 2005; *Gregory et al.*, 2005], or recent decline observed in the North Atlantic subpolar gyre [*Häkkinen and Rhines*, 2004]. Several ocean models have been forced by atmospheric reanalysis forcings, but these forcings have significant uncertainties and well-known heterogeneities over the last 50 years. The main model deficiencies lie in formulation of subgrid-scale mixing with consequences on deep-water formation, usually impacting the overturning circulation on the long term. In situ data assimilation in such models on long time scales requires complex tools and delicate choices on the method, that largely influence the results.

On the other hand, to avoid the need for accurate surface fluxes of heat and freshwater, one can use the observed temperature and salinity (TS) fields. Density providing the baroclinic velocities through the thermal wind relation, the barotropic part is obtained from the vorticity equation forced by the wind and a bottom pressure torque [*Sarkisyan and Keonjiyan*, 1975]. *Mellor et al.* [1982] integrated this equation along f/H contours, whereas *Holland and Hirschman* [1972] used the dynamical part of numerical ocean models, although some adjustment of the bottom density field may be necessary [*Ezer and Mellor*, 1994]. These methods have been applied to compare the pentads 1955-59 and

1970-74 [*Greatbatch et al.*, 1991; *Ezer et al.*, 1995], and more recently for 7 pentads from 1950 to 1994 using a finite element formulation [*Myers et al.*, 2005].

NODC has made available global fields of TS pentadal anomalies from 1955-59 to 1994-98 based on hydrographic data: we will diagnose mean ocean currents from these fields to investigate the low-frequency variations of mass and heat transports in the North Atlantic. We use three simple, well-documented methods: constant tracers, robust diagnostic, and short prognostic. Although the methods provide different results on the mean state, the low-frequency variations are rather coherent: these are illustrated in terms of poleward heat transport and compared with previously published results.

2. Model, Method and Datasets

The Regional Ocean Modeling System ROMS [*Shchepetkin and McWilliams*, 2005] is used, based on topography-following sigma coordinates. A smoothed bottom topography is required for accurate calculations of pressure gradients [*Barnier et al.*, 1998]. We used a 1/2° resolution and 50 sigma levels to reproduce correctly the ocean bottom topography and capture the signature of the boundary currents in the TS climatologies. The model configuration spans from 10°N to 66°N in the Atlantic. The model is used to produce mean fields of T, S and velocities for each 5-yr period from 1955-59 to 1994-98. The initial TS fields were optimally interpolated on the model grid from the pentadal fields available on a 1°×1° grid and 33 z-levels. These pentadal fields were constructed from objectively analyzed anomalies of T and S down to 3000 m [*Levitus et al.*, 2005; *Boyer et al.*, 2005] and from the associated mean climatology (down to the bottom). Wind stress and surface fluxes are provided by the atmospheric reanalyses from NCEP [*Kalnay et al.*, 1996] and ECMWF ERA-40 [*Uppala et al.*, 2005], averaged over the corresponding 5-yr periods.

Three semi-diagnostic methods are implemented. Constant Tracers (hereafter CT): T and S are kept constant during the model integration, only the momentum equations are integrated in time and reach a steady state within months [*Holland and Hirschman*, 1972]; the final velocity fields are averaged over months 6 to 12. Robust Diagnostic (RD): the tracer equations are now integrated in time with an additional relaxation to initial values with a timescale of 30 days [*Sarmiento and Bryan*, 1982]; kinetic and potential energy adjusts within 6 months, and the final fields are averaged over the second year of integration. Short Prognostic (PR): the full dynamics and tracer equations are integrated for 45 days such that the barotropic velocities adjusts but the tracers do not drift away from the initial state [*Ezer and Mellor*, 1994]; the final fields are averaged over the days 31 to 45. Rms differences between the initial and final TS fields are similar for both RD and PR methods (around 0.3 K at 100 m, 0.05 K at 1000 m and less than 0.01 K below 2000 m), although the former is in steady-state while the latter drifts rapidly from the initial state and longer prognostic integration would lead to much larger differences. Because the use of annual mean fields instead of seasonal cycle may be arguable, we have tested that the diagnostic transports of mass and heat on the annual mean climatology very closely resemble the mean of these diagnostics for the seasonal climatologies.

3. Mean Circulation and Transports

The three methods are first compared with the same TS fields from the mean climatology, and the same surface forcings averaged from the 40 years of ERA-40. These solutions do not differ significantly from the time-average of the pentad solutions. The CT method leads to the highest level of kinetic energy, associated with stronger barotropic gyres; the weakest barotropic circulation is for the PR method, which may not allow sufficient time to fully spin up the gyres. One weakness of the CT method is to generate a noisy barotropic circulation with large recirculations around topographic features, which are efficiently reduced through the adjustment of the density field with PR and RD methods.

For all methods, the poleward heat transport (PHT) shows a marked minimum around 42N at the intergyre (Fig. 1a), likely due, at least in part, to the missing eddy contribution to the heat transport [*Gulev et al.*, 2003]. The RD method leads to the highest values, especially in the subpolar gyre with more than 0.7 PW, whereas typical values of 1 PW are reached in the subtropical gyre. The largest discrepancies are found in the tropical region, where the CT method shows a striking minimum around 19°N (due to large southward barotropic contributions over slopes), and poleward of 38N where the RD method is largely above the others (due to both a strong subtropical barotropic gyre and a pronounced poleward eastern boundary current along the european shelf, and a larger overturning). These transports are in reasonable agreement with estimated mean transports from inversions [*Ganachaud and Wunsch*, 2003] and synoptic hydrographic sections [*Lumpkin et al.*, 2008].

4. Variability in Poleward Heat Transport

Standard deviation of PHT decreases from 10N to 35N, with a maximum around 42N, and decreases again poleward. The CT method shows a spurious maximum around 23N due to extremely high variability of the barotropic recirculation gyre around the seamount centered at 21N 31W, hence we will focus on results from the RD method in the following. Hövmoller diagrams of the heat transport anomalies (Fig. 1b) show an opposition of phase between the subtropical and subpolar gyres, with correlation coefficients reaching –0.6 to –0.8 between 22-25N and 48-54N (i.e. around the locations of the mean PHT extrema); this is in good agreement with the first EOF for PHT found in the 1993-2003 ECCO assimilation product [*Cabanes et al.*, 2008], but shown here to be valid on a much longer period. In the subtropical gyre, large PHT occured in the late 60's to mid 70's, and then in mid 80's, whereas low PHT occured around 1965, 1980 and 1995. At 25N, these variations are well correlated with the overturning circulation (r=0.82) which contribution dominates the PHT, but not with the barotropic gyre. In the subpolar gyre, all methods show the same variability (Fig. 2): large values of mass and heat transports in the 60's and the 90's, and low values in the 70's. PHT variability is mostly due to changes in meridional velocities rather than temperatures, except in the intergyre region (at 48N, correlations with $v'\overline{T}$ and $\overline{v}T'$ contributions are respectively 0.86 and 0.22). In the subpolar gyre, variations of the depth-averaged components control the PHT; at 48N correlations are slightly larger with the barotropic gyre intensity than with the overturning (0.87 vs 0.81).

5. Sensitivity Experiments

The use of NCEP or ECMWF 5-yr averaged surface fluxes leads to minor differences in the ocean variability; additional series of experiments were forced with the 40-yr-averaged ERA-40 surface fluxes and show identical variations (Fig. 2). On 5-yr time scales that filter out a large part of the North Atlantic Oscillation (NAO) interannual variability, the influence of surface fluxes variations appear negligible in the variations of the circulation obtained with our methods. This confirms that the influence of the changing forcing is largely imprinted in the interannual thermohaline fields, and that changes in the barotropic circulation are mainly related to changes in the JEBAR term and not the Ekman pumping.

Finally, we estimate the influence of the vertical extent of the interannual TS variations by performing three additional series of experiments (RD method) with variable TS fields down to 2000, 1000 and 0m (i.e. only the surface forcing is modified between pentads): the correlation coefficients for the maximum PHT in the subpolar gyre with the control experiment (TS variable down to 3000m) are respectively 0.99, 0.90 and –0.05. Consequently, we expect that the variations of such diagnostics will be very well represented from interannual fields reconstructed from the Argo floats array profiling down to 2000m.

6. Comparison with Previous Results

Greatbatch et al. [1991] have diagnosed the barotropic streamfunction following *Mellor et al.* [1982] method for the pentads 1955-59 and 1970-74, and found a Gulf Stream 30 Sv weaker in the latter period. Our results show similar changes but with a weaker amplitude (22 Sv) and more intense smaller scale patterns, in better agreement with the diagnostic and short-term prognostic models results of *Ezer et al.* [1995]. Their PHT variations agree also with ours: increased (decreased) PHT in the subtropical (subpolar) gyre in the 70's compared to the 50's, by more than 0.1 PW. In contrast *Greatbatch and Xu* [1993] computed reduced PHT by 0.2 PW through both sections at 54N and 24N using thermal wind velocities referenced to the bottom: mass balance was achieved with absolute transport from *Greatbatch et al.* [1991] resulting in a method very similar to CT at 54N, but traditional hydrographic method imposing the Florida Current transport at

24N. *Sidorenko et al.* [2008] recently performed inverse calculations of the North Atlantic circulation using 7 pentadal TS fields from 1960 to 1994: variations of the barotropic streamfunction show a larger amplitude in our results, but the first EOF pattern and time series (not shown) compare very well and support enhanced subtropical gyre transport following high NAO index periods.

Comparison with a 1958-2001 hindcast simulation of the state-of-the-art global 1/4° model ORCA025-G70 from the Drakkar project [*Barnier et al.*, 2006] with an ERA-40 based atmospheric forcing show very similar low-frequency variability of the subpolar heat transport, with maximum values in 1960 and 1996, and minimum in 1972 (Fig. 2a). These variations compare very well with those of *Eden and Willebrand* [2001] and *Eden and Jung* [2001] at 48N. Similar coordinated intensification of the horizontal and vertical subpolar gyre mass transports from 1970 to 1995 are also obtained by *Böning et al.* [2006] and *Deshayes and Frankignoul* [2008] with models of resolution varying from 1/3° to 1/12°.

These variations in the subpolar gyre transports are in relatively good agreement with the transport index of *Curry and McCartney* [2001]: the timing of our 70's minimum is delayed by a few years, but we cannot expect a precise correspondence from pentadal fields. These changes have been interpreted as an integrated response to the low-frequency variations of the NAO, the associated overturning changes being related to the convection in the Labrador Sea [*Latif et al.*, 2006]. *Eden and Jung* [2001] suggest that, in response to the variations of surface heat forcing related to the NAO, both the overturning and the barotropic streamfunction in the subpolar gyre (hence PHT) respond in phase within 3–5 yr due to baroclinic processes. Such relation between horizontal and vertical cells is also advocated by *Häkkinen and Rhines* [2004] through the changes in the Labrador Sea thermohaline structure associated with deep convection. Our results are in good agreement with such a mechanism.

7. Summary and Perspective

This work provides an estimate of the low-frequency variability in the North Atlantic circulation based on in situ TS data using simple methods: diagnostic, robust-diagnostic and short prognostic. Without finely tuning the model configuration or parametrizations, the variability in mass and heat transports associated with the thermohaline changes has been sucessfully captured in the subpolar gyre, as compared to state-of-the-art prognostic models: energetic barotropic and overturning circulations drive high heat transport in the early 60's and mid 90's, whereas both circulations and heat transport are at the lowest in the mid 70's, in agreement with observational estimates attributed to NAO forcing [*Curry and McCartney*, 2001]. Our methods also point out an apparent phase opposition in heat transport between the subtropical and subpolar gyres, that could result from the delayed adjustement of the meridional overturning at lower latitude to the low-frequency NAO forcing [*Eden and Jung*, 2001]. The original idea of relying on in situ observations rather than changes in the surface forcing to investigate the variations of the ocean circulation provides an alternative to prognostic hindcast models, with or without assimilation, that avoids potential model drift associated with uncertainties in both subgrid-scale processes parameterizations and surface fluxes. The variability of the surface forcing is clearly of second-order influence, as shown by *Ezer et al.* [1995] for the wind-stress. The three methods show different strengths and weaknesses. CT is the most straightforward, closer to observations, but leads to noisy velocity fields [*Ezer et al.*, 1995], associated with strong localized barotropic recirculations around seamounts. Both RD and PR have an arbitrary parameter, respectively the restoring time scale and the integration time. For the choices made here, both methods lead to similar rms differences between the final and initial TS fields, the RD method providing a steady-state as compared to PR continuous drift. Let us recall that these are dynamical and not thermodynamical methods: they allow only limited insight in heat or salt budgets for instance.

The pentadal TS fields are certainly not perfectly constrained over the four decades, especially at depth, and due to the scarcity of salinity data: the robustness of our results is now investigated with the use of alternative products (hydrobase), analyzed on isopycnal surfaces and/or based on longer time periods. The large smoothing in the NODC dataset, as discussed in *Myers et al.* [2005], may also have some influence on our results, especially with the CT method. A radical change occured in the observing system since 2003 with Argo, that allows to build reliable annual fields of TS for the upper 2000m, and we have shown this will be sufficient to reconstruct most of the large-scale circulation changes. The next step is to implement these methods in a global configuration, and use updated TS fields to investigate the more recent changes of the general circulation.

Acknowledgments. The assistance of P. Marchesiello and P. Penven with ROMS and their development of the friendly IRD version including pre- and post-processing package are gratefully acknowledged. Pentadal TS anomalies have been downloaded from the NODC website. ECMWF ERA-40 and NCEP reanalysis data used in this study have been obtained freely from their respective data server.

References

Barnier, B., et al. (1998), A sigma-coordinate primitive equation model for studying the circulation in the South Atlantic. Part I: Model configuration with error estimates, *Deep-Sea Res. Part I*, *45*, 543–572.

Barnier, B., et al. (2006), Impact of partial steps and momentum advection schemes in a global ocean circulation model at eddy permitting resolution, *Ocean Dynamics*, *56*, 1616–7341, doi:10.1007/s10236-006-0082-1.

Böning, C. W., et al. (2006), Decadal variability of subpolar gyre transport and its reverberation in the North Atlantic overturning, *Geophys. Res. Lett.*, *33*, L21S01, doi: 10.1029/2006GL026906.

Boyer, T. P., et al. (2005), Linear trends in salinity for the world ocean, 1955-1998, *Geophys. Res. Lett.*, *32*, L01604, doi:10.1029/2004GL021791.

Bryden, H. L., H. R. Longworth, and S. A. Cunningham (2005), Has the Atlantic overturning circulation slowed?, *Nature*, *438*, 655–657.

Cabanes, C., T. Lee, and L.-L. Fu (2008), Mechanisms of interannual variations of the meridional overturning circulation of the North Atlantic Ocean, *J. Phys. Oceanogr.*, *38*, 467–480.

Curry, R. G., and M. S. McCartney (2001), Ocean Gyre Circulation Changes Associated with the North Atlantic Oscillation, *J. Phys. Oceanogr.*, *31*, 3374–3400.

Deshayes, J., and C. Frankignoul (2008), Simulated variability of the circulation in the North Atlantic from 1953 to 2003, *J. Clim.*, *21*, 4919–4933.

Dickson, B., et al. (2002), Rapid freshening of the deep North Atlantic Ocean over the past four decades, *Nature*, *416*, 832–837.

Dickson, R., et al. (1996), Long-term coordinated changes in the convective activity of the North Atlantic, *Prog. Oceanogr.*, *38*, 241–295.

Eden, C., and T. Jung (2001), North Atlantic interdecadal variability: Oceanic response to the North Atlantic Oscillation (1865-1997), *J. Clim.*, *14*, 676–691.

Eden, C., and J. Willebrand (2001), Mechanism of Interannual to Decadal Variability of the North Atlantic Circulation., *J. Clim.*, *14*, 2266–2280.

Ezer, T., and G. L. Mellor (1994), Diagnostic and prognostic calculations of the North Atlantic circulation and sea level using a sigma coordinate ocean model, *J. Geophys. Res.*, *99*, 14,159–14,172.

Ezer, T., G. L. Mellor, and R. J. Greatbatch (1995), On the interpentadal variability of the North Atlantic Ocean: Model simulated changes in transport, meridional heat flux and coastal sea level between 1955-1959 and 1970-1974, *J. Geophys. Res.*, *100*, 10,559–10,566.

Ganachaud, A., and C. Wunsch (2003), Large-scale ocean heat and freshwater transports during the World Ocean Circulation Experiment, *J. Clim.*, *16*, 696–705.

Greatbatch, R. J., and J. Xu (1993), On the transport of volume and heat through sections across the North Atlantic: Climatology and the pentads 1955-1959, 1970-1974, *J. Geophys. Res.*, *98*, 10,125–10,142.

Greatbatch, R. J., A. F. Fanning, A. Goulding, and S. Levitus (1991), A diagnosis of interpentadal circulation changes in the North Atlantic, *J. Geophys. Res.*, *96*, 22,009–

22,023.

Gregory, J. M., et al. (2005), A model intercomparison of changes in the Atlantic thermohaline circulation in response to increasing atmospheric CO2 concentration, *Geophys. Res. Lett.*, *32*, L12703.

Gulev, S. K., et al. (2003), Water transformation in the North Atlantic and its impact on the meridional circulation: insights from an ocean model forced by NCEP-NCAR reanalysis surface fluxes, *J. Clim.*, *16*, 3085–3110.

Häkkinen, S., and P. B. Rhines (2004), Decline of subpolar North Atlantic circulation during the 1990s, *Science*, *304*, 555–559.

Holland, W. R., and A. D. Hirschman (1972), A numerical calculation of the circulation in the North Atlantic Ocean, *J. Phys. Oceanogr.*, *2*, 336–354.

Kalnay, E., et al. (1996), The NCEP/NCAR 40-year reanalysis project, *Bull. Am. Met. Soc.*, *77*, 437–471.

Latif, M., et al. (2006), Is the thermohaline circulation changing?, *J. Clim.*, *19*, 4631–4637.

Levitus, S., J. I. Antonov, and T. P. Boyer (2005), Warming of the World Ocean, 1955-2003, *Geophys. Res. Lett.*, *32*, L02604, doi:10.1029/2004GL021592.

Lumpkin, R., K. Speer, and K. P. Koltermann (2008), Transport across 48°N in the North Atlantic Ocean, *J. Phys. Oceanogr.*, *38*, 733–752.

Mellor, G. L., C. R. Mechoso, and E. Keto (1982), A diagnostic calculation of the general circulation of the Atlantic Ocean, *Deep-Sea Res.*, *29*, 1171–1192.

Myers, P. G., S. Grey, and K. Haines (2005), A diagnostic study of interpentadal variability in the North Atlantic Ocean using a finite element model, *Ocean Model.*, *10*, 69–81.

Sarkisyan, A. S., and V. P. Keonjiyan (1975), *Review of numerical ocean circulation models using the observed density field*, pp. 76–93, Numerical Models of Ocean Circulation, National Academy of Sciences, Washington D.C., USA.

Sarmiento, J. L., and K. Bryan (1982), An ocean transport model for the North Atlantic, *J. Geophys. Res.*, *106*, 16,711–16,728.

Shchepetkin, A., and J. C. McWilliams (2005), The Regional Oceanic Modeling System: A split-explicit, free-surface, topography-following-coordinate ocean model, *Ocean Model.*, *9*, 347–404.

Sidorenko, D., S. Danilov, and J. Schröter (2008), Inverse solution for pentadal variability in the north atlantic, *Geophys. Res. Lett.*, *35*, L02603, doi:10.1029/2007GL032463.

Uppala, S. M., et al. (2005), The ERA-40 re-analysis, *Q. J. R. Meteorolog. Soc.*, *131*, 2961–3012.

Figure 1. (a) Poleward heat transport averaged over 1955-1998 from pentadal fields (solid), and computed for the mean TS climatology and mean ERA-40 surface fluxes (dashed), for the 3 methods: robust diagnostic (RD), constant tracers (CT), short prognostic (PR), and for the global prognostic simulation ORCA025-G70 (1958-2001). (b) PHT anomaly (PW) computed from the pentadal TS anomalies and ERA-40 5-yr average surface fluxes, with the RD method.

Figure 2. (a) PHT maximum in the subpolar gyre (45-60°N) computed from the pentadal TS anomalies for the 3 methods and various forcing: ERA-40 (solid) or NCEP (dashed) 5-yr average surface fluxes, ERA-40 40-yr-averaged fields (dash-dotted); the additional curves are for the global prognostic simulation ORCA025-G70 annual and pentadal means. (b) Thermohaline circulation and (c) barotropic subpolar gyre intensity at 48N for the RD method.

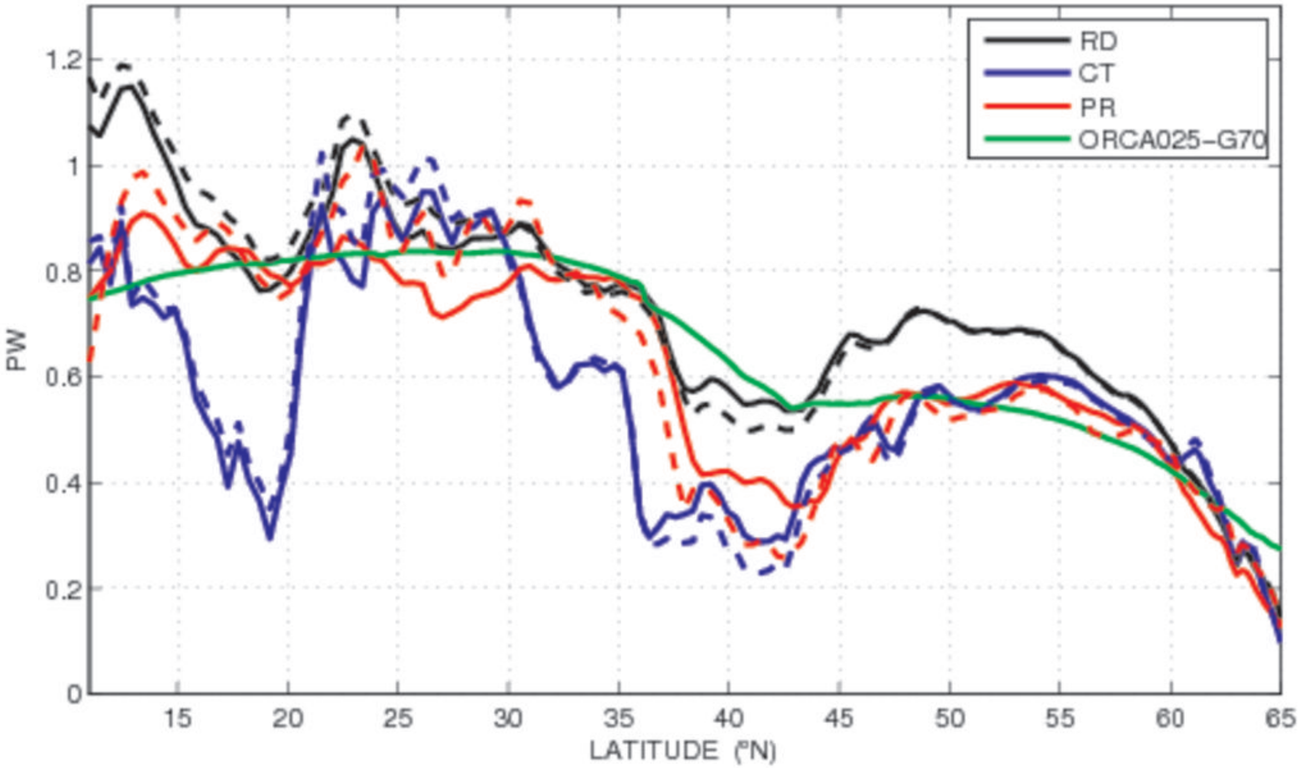
RD
CT
PR
ORCA025-G70
PW
0
0.2
0.4
0.6
0.8
1
1.2
15
20
25
30
35
40
45
50
55
60
65
LATITUDE (°N)

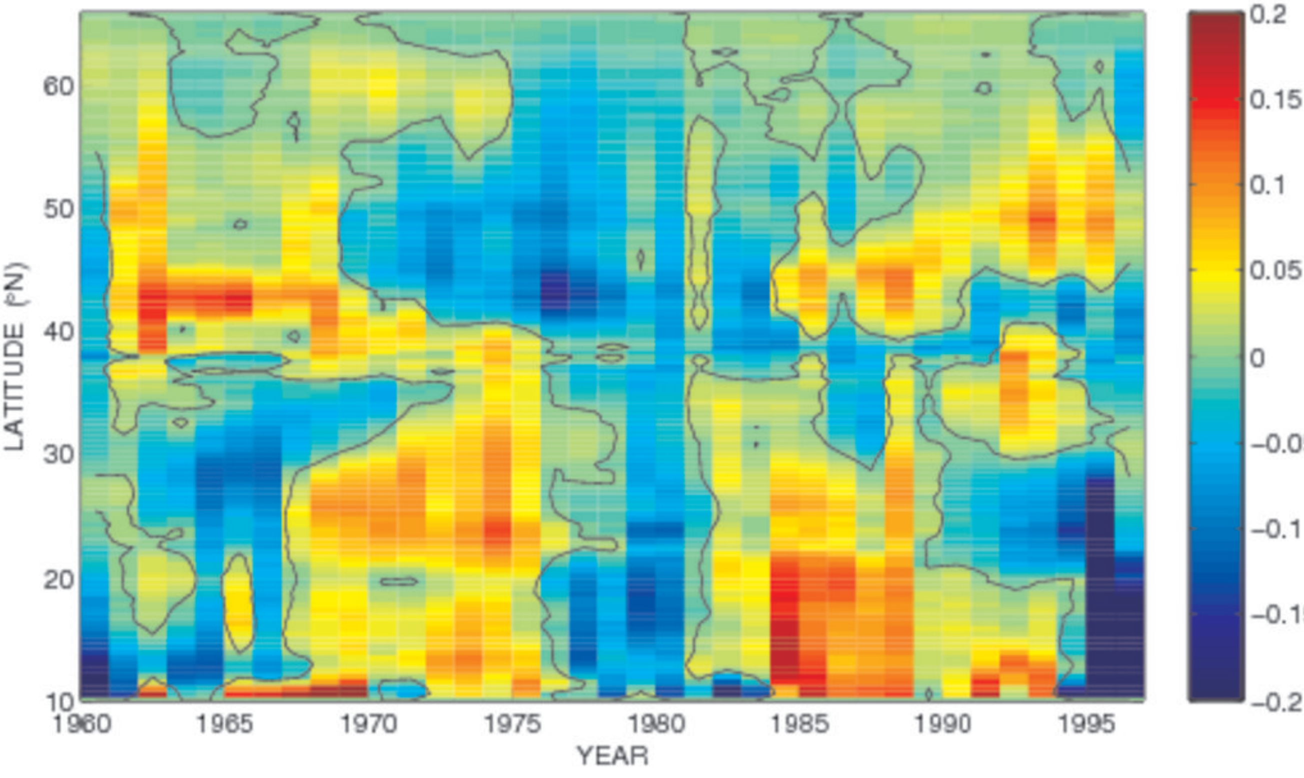
LATITUDE (°N)
10
20
30
40
50
60
1960
1965
1970
1975
1980
1985
1990
1995
YEAR
0.2
0.15
0.1
0.05
0
−0.05
−0.1
−0.15
−0.2

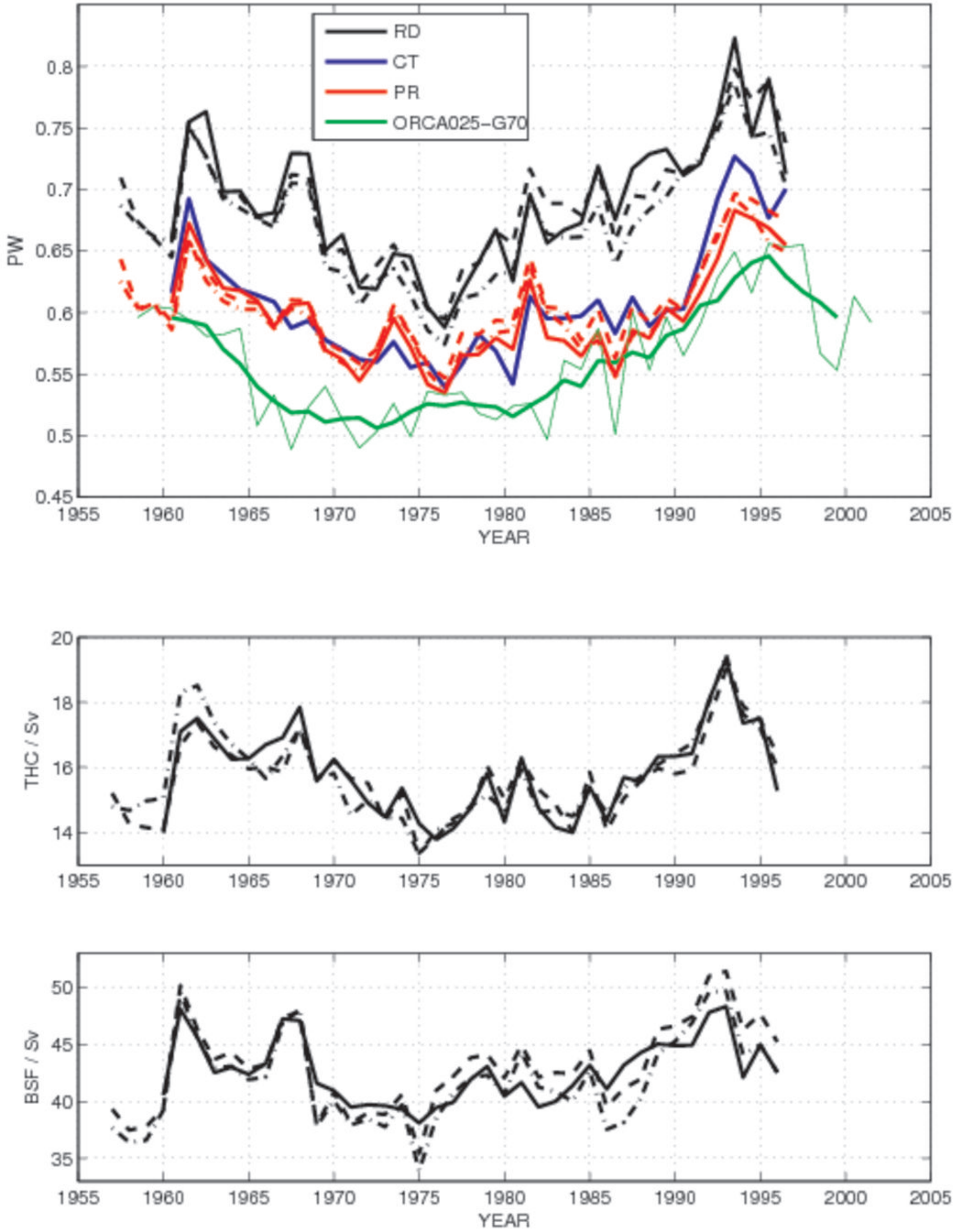RD
CT
PR
ORCA025-G70
PW
0.45
0.5
0.55
0.6
0.65
0.7
0.75
0.8
1955
1960
1965
1970
1975
1980
1985
1990
1995
2000
2005
YEAR
THC / Sv
14
16
18
20
1955
1960
1965
1970
1975
1980
1985
1990
1995
2000
2005
BSF / Sv
35
40
45
50
1955
1960
1965
1970
1975
1980
1985
1990
1995
2000
2005
YEAR